Cox6a2 is a thrifty gene that predisposes to high fat diet-induced obesity and glucose intolerance in mice

Roel Quintens[1], Sarvjeet Singh[2], Katleen Lemaire[1], Katrien De Bock[3], Anica Schraenen[1], Berthe Van Hoef[4], Irene Vroegrijk[5], Pieter Van Noten[6], Stefan Lehnert[1], Mikaela Granvik[1], Leentje Van Lommel[1], Lieven Thorrez[1], Nico Hendrickx[1], J.A. Romijn[5], Roger Lijnen[4], Peter J. Voshol[5], Pradeep P.A. Mammen[2], Frans C. Schuit[1,*]

[1] Gene Expression Unit, Department of Molecular Cell Biology, Katholieke Universiteit Leuven, Herestraat 49, box 901, 3000 Leuven, Belgium.

[2] Division of Cardiology, Department of Internal Medicine, University Hospital-St. Paul, University of Texas Southwestern Medical Center, Texas, USA.

[3] Vesalius Research Center, VIB – Katholieke Universiteit Leuven, Herestraat 49, box 912, 3000 Leuven, Belgium.

[4] Center for Molecular and Vascular Biology, Katholieke Universiteit Leuven, Herestraat 49, box 911, 3000 Leuven, Belgium.

[5] Department of Endocrinology and Metabolic Diseases, Leiden University Medical Center, Leiden, The Netherlands.

[6] Physical Activity and Health Laboratory, Biomedical Kinesiology Department, FaBeR, Katholieke Universiteit Leuven, Tervuursevest 101, 3001 Leuven, Belgium

[*] Correspondence: Frans.Schuit@med.kuleuven.be

Summary

Interaction between thrifty genotypes and a Western lifestyle may explain the pandemia of obesity and type 2 diabetes of the modern world. However, molecular examples of this interaction have not been worked out in detail, and the concept of thrifty genes is currently debated. In this paper, we show that mice deficient in the CoxVIaH subunit of cytochrome c oxidase ($Cox6a2^{-/-}$ mice) are sensitive to food deprivation, losing body weight more rapidly than control mice, and having enhanced basal metabolism. Mechanistically, these changes are explained by uncoupling of oxidative phosphorylation via increased UCP1 and UCP2 expression. In agreement with the thrifty gene hypotyhesis, $Cox6a2^{-/-}$ mice were completely resistant to high fat diet-induced obesity and insulin resistance. Thus, Cox6a2 fulfills all criteria of a thrifty gene as it links overall efficiency of energy homeostasis to diet-induced obesity and insulin resistance by regulating UCP expression.

Introduction

The current pandemia of obesity and type 2 diabetes is ascribed to a detrimental interaction between a Western lifestyle and gene polymorphism(s) that were selected in our ancestors and are now common in many human populations. About 50 years ago, it was proposed that obesity and type 2 diabetes are predisposed by "thrifty genes" that allow efficient storage and utilization of energy when food was abundant (NEEL, 1962). A thrifty genotype thus confers a survival benefit on the individual during periods of famine and it was suggested that such genes were commonly subject of intense evolutionary pressure. In today's Western society, where calorie-dense food is omnipresent and abundant, "thrifty genotypes" are deleterious as they promote fat deposition for a famine that never comes, resulting in obesity and obesity-related diseases such as insulin resistance and type 2 diabetes. Since it provided a genetic basis for type 2 diabetes, the thrifty gene hypothesis has been influential since it was published. However, untill now, only very few examples of thrifty genes have been proposed (Auwerx, 1999; Tabarin et al., 2005), with sparce experimental evidence, so that opposition against the concept is growing (Speakman, 2006; Speakman, 2007; Speakman, 2008).

Obesity develops when energy intake (feeding) chronically exceeds energy expenditure (basal metabolism, physical activity, and adaptive thermogenesis) (Lowell and Spiegelman, 2000; Puigserver et al., 1998). Obesity often predisposes to the development of insulin resistance and diabetes, and therefore

inducing weight loss by promoting a healthy lifestyle is often used as an initial therapeutic intervention for obese type 2 diabetics. However, these strategies have only short-term success and are unsucessfull in 95% of the cases at long-term (Crawford et al., 2000). Thus, it is proposed that long-term strategies for inducing weight loss should aim at increasing the patients' metabolic rates by decreasing their metabolic efficiency (Choi et al., 2007). This can be achieved in mice by direct or indirect induction of uncoupling proteins which dissociate oxidative phophorylation from ATP synthesis and dissipate energy as heat (Choi et al., 2007; Clapham et al., 2000; Gates et al., 2007; Li et al., 2000; Polak et al., 2008).

Complex IV of the respiratory chain (cytochrome c oxidase; COX) is the site where oxygen is reduced as a common endpoint of carbohydrate and fatty acid oxidation in most eukaryotic cells. One of its thirteen subunits, CoxVIa, is believed to be important for the assembly as well as for regulation of the catalytic properties of the core subunits of the complex. CoxVIa is expressed as two different isoforms, CoxVIaL (liver-type), and CoxVIaH (heart-type), encoded by the *Cox6a1* and *Cox6a2* genes, respectively. CoxVIaL is ubiquitously expressed, whereas expression of CoxVIaH is restricted to striated muscle (Kadenbach et al., 1995; Taanman et al., 1993). The CoxVIaH (but not CoxVIaL) subunit has been shown to bind ADP and ATP (Tsukihara et al., 1996); binding of ADP results in increased catalytic activity which can be abolished by competition with monoclonal antibodies (Anthony et al., 1993). However, at high intramitochondrial ATP/ADP ratios (i.e. at rest), reconstituted bovine heart COX

was shown to have decreased proton pumping capacity, also called "slip" (Frank and Kadenbach, 1996). This intrinsic uncoupling mechanism has been suggested to play a role in thermogenesis in heart and skeletal muscle at rest (Rohdich and Kadenbach, 1993; Lowell and Spiegelman, 2000). Slipping of cytochrome c oxidase has also been proposed to protect against the formation of mitochondrial reactive oxygen species (ROS) (Papa et al., 1997).

Whole body CoxVIaH deficient mice ($Cox6a2^{-/-}$ mice) are viable and have been reported to have a mild cardiac dysfunction resulting in decreased stroke work (Radford et al., 2002). Because of the specific regulatory properties of CoxVIaH in oxidative phosphorylation, we studied in this paper whole body energy metabolism and insulin sensitivity of $Cox6a2^{-/-}$ mice. The results indicate that the absence of the *Cox6a2* gene has a profound influence on energy expenditure and thermogenesis: $Cox6a2^{-/-}$ mice rapidly lose body weight upon short-term fasting and are completely protected against diet-induced obesity through a mechanism including increased ROS formation and expression of uncoupling proteins (UCPs) in muscle. Thus, we propose that *Cox6a2* fullfils the criteria of a thrifty gene which promotes efficient storage and utilization of energy and which predisposes to diet-induced obesity and insulin resistance.

Results

Cox6a2$^{-/-}$ mice lose more body weight upon short-term fasting and are resistant to cold temperature.

As the CoxVIaH subunit of the respiratory chain regulates intrinsic uncoupling of oxidative phosphorylation (Frank and Kadenbach, 1996) we studied the metabolic phenotype of mice that are deficient in CoxVIaH protein (Cox6a2$^{-/-}$ mice). As is illustrated in Figure 1, both male and female Cox6a2$^{-/-}$ mice are hypersensitive to 36h of fasting in that they lose significantly more weight as compared to wild-type animals. Moreover, two of the Cox6a2$^{-/-}$ males had to be refed after 24 h, because they were moribund. Between 24 h and 36 h of fasting, the calculated average weight loss in the male Cox6a2$^{-/-}$ mice (slope = -0.52 ± 0.03 % weight loss per h) was almost twice as high as in the male controls (slope = -0.28 ± 0.02 %; $p < 0.001$). This period corresponds to the "coping phase" of body weight loss, in which primarily fat and ketone bodies are used as an energy source (Sokolovic et al., 2007). This result indicates that expression of CoxVIaH renders mice more resistant to fasting, preventing excessive body weight loss and early onset of lethargy. To better understand the dynamics of the *Cox6a2* gene in response to the fasted state, we next determined Cox6a2 mRNA levels after overnight fasting in wild-type mice. Indeed, we found that in soleus muscle Cox6a2 mRNA expression was increased more than 3-fold after 16 hours of fasting (Figure 1C). While no increase was seen in diaphragm or in gastrocnemius muscle (slight decrease), the strong upregulation of Cox6a2

mRNA in soleus muscle (slow-oxidative) indicates that CoxVIaH participates in the physiological response to fasting. To test if basal energy metabolism was responsible for the enhanced body weight loss during fasting, we next challenged the mice with a cold (4°C) environment and followed body temperature. Both in mice that were fed a regular diet (Figure 1D) as in animals on high fat diet (HFD) (Figure 1E) body temperature remained more constant in Cox6a2$^{-/-}$ mice, likely because of enhanced non-shivering thermogenesis. This result was unexpected, since CoxVIaH has been suggested to play a role in thermogenesis at rest (Lowell and Spiegelman, 2000; Rohdich and Kadenbach, 1993). To rule out a compensation mechanism via the thyroid-pituitary axis, we also assessed thyrotropin (TSH) bioactivity (which is a measure for TSH content) and plasma T_4 levels: both hormones were not significantly changed in Cox6a2$^{-/-}$ mice (Figure S1), suggesting that the thyroid-pituitary axis is not responsible for the increased thermogenesis we observed in Cox6a2$^{-/-}$ mice.

Energy expenditure and heat generation are increased in Cox6a2$^{-/-}$ mice

In the next experiment we tested if increased overall basal metabolic rate was responsible for the accelerated weight loss during fasting and the resistance to cooling in a cold environment. We therefore performed indirect calorimetric measurements on mice fed a regular diet. We found that Cox6a2$^{-/-}$ mice consumed more oxygen and generated more heat during the day, i.e. when they were more active (Figure 2A and 2C). During the night, there was only a small,

non-significant increase in oxygen consumption and heat generation, despite a 25% decrease in spontaneous activity (Figures 2D and 2E). There was no difference between wild-type and Cox6a2$^{-/-}$ mice in the respiratory exchange ratio (RER) (Figure 2B), suggesting that fat metabolism is unaltered, at least on a regular diet. Total food intake was similar between Cox6a2$^{-/-}$ and wild-type mice, but the daily intake of water was slightly lower in Cox6a2$^{-/-}$ mice (Figure S2B). Together, these data show that Cox6a2$^{-/-}$ mice convert significantly more stored energy into heat, indicating that CoxVIaH may be an important regulator for whole-body metabolic rate.

UCP2 expression is elevated in skeletal muscle and adipose tissue of Cox6a2$^{-/-}$ mice

Because of their potential role in the regulation of overall energy expenditure, we measured mRNA expression of uncoupling proteins (UCPs) as well as their transcription factors PGC-1α and PPAR-α in major metabolically active tissues such as skeletal muscle, heart, white adipose tissue (WAT) and brown adipose tissue (BAT). We studied diaphragm, as well as the gastrocnemius and soleus muscles to distinguish between glycolytic versus slow and fast oxidative muscle types. In addition, we studied adipose tissue for the UCP's and quantified expression of the second CoxVIa isoform, CoxVIaL. Generally, the expression of UCP2 was significantly increased in Cox6a2$^{-/-}$ mice (Figure 3A), but there were tissue-specific effects. A modest 2 to 3-fold increase was observed in gastrocnemius and soleus muscle, and adipose tissue; in contrast expression of

UCP2 was more than 10-fold increased in diaphragm of Cox6a2$^{-/-}$ mice. Consistent with this important change, diaphragm of Cox6a2$^{-/-}$ mice also expressed more of regulatory factors of UCP2 transcription, such as PGC-1α and PPARα (Figure 3A). In diaphragm of Cox6a2$^{-/-}$ mice we also found a compensatory increase of Cox6a1 mRNA and a 6-fold decrease in UCP3 mRNA when compared to wild type mice. Finally, diaphragm, soleus muscle and heart of Cox6a2$^{-/-}$ mice also upregulated the expression of UCP1 between 4- to 9-fold (Figure 3A), whereas in white adipose tissue of high fat diet fed Cox6a2$^{-/-}$ mice, UCP1 expression was increased 3-fold (Figure S3). Together, these results show that expression of UCP2 and to a lesser extent also UCP1 is induced in muscle and adipose tissue of Cox6a2$^{-/-}$ mice, and they suggest that the induction of a constitutive uncoupling mechanism may be responsible for the enhanced metabolic rate of these animals.

Ablation of Cox6a2$^{-/-}$ results in increased production of reactive oxygen species in skeletal muscle

Slipping or intrinsic uncoupling of oxidative phosphorylation has been proposed to protect against the formation of ROS (Papa et al., 1997). It is also known that ROS can induce the expression (Lee et al., 1999; Yang et al., 2000) as well as the activity of uncoupling proteins (Echtay et al., 2002a; Echtay et al., 2002b). Moreover, without ROS as activators, UCPs are not functional (Brand et al., 2004a; Brand et al., 2004b). To assess if elevated expression of UCPs in

Cox6a2$^{-/-}$ mice could be caused by increased ROS generation, we measured steady state ROS levels in diaphragm and hindlimbs of Cox6a2$^{-/-}$ and wild-type mice via dihydroethidium (DHE) (Zanetti et al., 2005). As can be seen in Figure 3B, elevated ROS levels were detected both in diaphragm and in hindlimb muscles from Cox6a2$^{-/-}$ mice but the difference was largest in diaphragm; this difference correlates well with the strongest induction of UCP2 in diaphragm, when compared to other tested muscle types (Figure 3A). This suggests that the increase in UCP2 mRNA expression in tissues of Cox6a2$^{-/-}$ mice occurs secondary to elevated generation of ROS.

Cox6a2-deficient mice have increased number of oxidative muscle fibers and improved resistance to muscle fatigue

Because muscle-specific effects were observed when comparing changes in ROS and UCP levels of wild-type *versus* Cox6a2$^{-/-}$ mice, we next performed microarrays to compare gene expression in gastrocnemius muscle and diaphragm of Cox6a2$^{-/-}$ and wild-type mice. Since most of the changes in mRNA expression were rather small, we used gene set enrichment analysis (GSEA) to look for statistically significant, coordinate changes in gene expression of a priori defined sets of genes. We found that both in gastrocnemius and diaphragm, expression of genes associated with mitochondrial function was elevated in Cox6a2$^{-/-}$ mice (Supplementary Table 1 and 2). Examples of such genes are nuclear encoded subunits of the respiratory chain (Figures 4A-C). As can be seen in figure 4C, expression of almost all transcripts encoding mitochondrial

respiratory chain subunits was moderately (between 10 and 70%) upregulated, especially in diaphragm. We also found an upregulation of markers for oxidative (type I, IIA) myofibers in both gastrocnemius and diaphragm of Cox6a2$^{-/-}$ mice. In contrast, markers for glycolytic (type IIB) myofibers were downregulated (Figures 4A and 4B, right panels). This indicates that in Cox6a2$^{-/-}$ mice, skeletal muscle fibers have switched to a slower, more oxidative phenotype. A skeletal muscle fiber type switch was confirmed by a metachromatic ATPase assay to screen for differences in the amount of type I, IIA, and IIB fibers. As can be seen in Figures 4C and 4D, we found that in gastrocnemius muscle of Cox6a2$^{-/-}$ mice there was an increase in the number of oxidative type IIA fibers. Moreover, the total number of myofibers per mm^2 was significantly increased in Cox6a2$^{-/-}$ gastrocnemius, and the cross sectional area of all fiber types in Cox6a2$^{-/-}$ mice was reduced. However, we did not observe a fiber type switch in diaphragm of Cox6a2$^{-/-}$ mice (data not shown). The switch in muscle fiber composition towards a slower profile in Cox6a2$^{-/-}$ mice was also reflected by the mechanic properties of these muscles. We found that the contractility of soleus and extensor digiti longissimus (EDL) muscle, as well as the grip strength were similar between wild-type and Cox6a2$^{-/-}$ mice of 16 weeks (Figures S4A and S4B). However, in a fatigue and recovery test, soleus muscle of Cox6a2$^{-/-}$ mice was better resistant to fatigue and recovered much faster compared to wild-type muscle (Figure S4C), consistent with an increase in oxidative muscle fibers. Together, our data indicate that, despite the reduced COX activity in Cox6a2$^{-/-}$ muscles, the switch of muscles to a more oxidative fiber type is sufficient not only to overcome this deficiency but

also to improve muscle function. Finally, despite the loss of CoxVIaH expression, ATP content of skeletal muscles of Cox6a2$^{-/-}$ mice and wild-type mice was similar (Figure S5), which is consistent with previous observations in heart (Radford et al., 2002). Thus, Cox6a2$^{-/-}$ mice have developed compensatory mechanisms that allow production of sufficient amounts of ATP to perform mechanical work.

Cox6a2$^{-/-}$ mice are lean and protected against diet-induced obesity

Many animal models with increased energy expenditure also display reduced body weight (Reitman, 2002). In agreement with this relationship, we found that, under standard feeding conditions, Cox6a2$^{-/-}$ mice developped a progressive decrease in body weight as compared to age- and sex-matched wild-type mice. When wild-type mice were fed a HFD, the animals became progressively obese, the difference with control fed mice of the same strain being significant already after 4 weeks of HFD feeding (Figure 5A). On the contrary, no weight gain above control diet was observed when Cox6a2$^{-/-}$ mice were fed a HFD (Figure 5A). Although Cox6a2$^{-/-}$ mice on a HFD ate less than wild-type mice (Figure 5B, left panel), the difference in weight gain between wild-type and knockout was mainly attributable to decreased feeding efficiency (Figure 5B, right panel). The difference in whole body weight after a HFD was primarily caused by increased adiposity in wild-type animals both in gonadal and subcutanous fat pads (Figure 5C). As expected from animals with a cardiomyopathy (Radford et al., 2002), we also observed slightly increased heart weights in Cox6a2$^{-/-}$ mice. The reduced

mass of the gonadal fat pad in Cox6a2$^{-/-}$ mice fed a HFD was associated with decreased adipocyte size and increased cellular density 12 weeks after start of HFD feeding (Figure 5D). A similar trend, but with smaller differences, was observed for adipocytes from subcutanous fat (Figure 5D). Together, these data show that in Cox6a2$^{-/-}$ mice a HFD fails to result in the extra fat storage in adipose tissue, that causes diet-induced weight gain in the control group.

Increased glucose tolerance and insulin sensititvity in Cox6a2$^{-/-}$ mice on a HFD

The diet-induced obesity in wild-type mice was associated with increased plasma levels of insulin, leptin, cholesterol and triglycerides compared to Cox6a2$^{-/-}$ mice (Supplementary Table 2). The difference in plasma insulin between wild-type and Cox6a2$^{-/-}$ mice despite similar random fed blood glucose levels indicated that a difference existed in insulin sensitivity. To test this, we first performed intraperitoneal glucose tolerance tests in mice that were either on regular diet or fed a HFD for 9 or 22 weeks. When fed a regular diet, we observed no difference in glucose tolerance between Cox6a2$^{-/-}$ and wild-type mice, although Cox6a2$^{-/-}$ mice did have significantly lower fasting glucose levels (Figure 6A, left panel). When fed a HFD, wild-type mice developed progressive glucose intolerance with marked degree of hyperglycemia two hours after glucose injection (Figure 6A); on the contrary, no difference in glucose tolerance was seen in Cox6a2$^{-/-}$ mice after 22 weeks of HFD *versus* regular diet (Figure 6A, right panel). To assess whether the preservation of glucose tolerance in Cox6a2$^{-/-}$ mice after HFD was a

result of increased insulin sensitivity, we performed hyperinsulinemic, euglycemic clamps on mice fed a HFD for 15 weeks. Upon infusion of insulin, Cox6a2$^{-/-}$ mice immediately showed a substantial drop in blood glucose levels, requiring significantly more glucose to maintain glucose levels which, moreover, were significantly lower than those in wild-type mice (Figure 6B). We also performed clamps on mice that were fed a regular diet. Unfortunately, four out of five Cox6a2$^{-/-}$ mice died during the experiment, presumably as a result of hypertension because too much of the glucose solution had to be injected to maintain blood glucose levels. Average glucose levels of these mice at the time of death was 42 $\pm$ 5 mg/dl, which is below normoglycemia. These results show that Cox6a2$^{-/-}$ mice indeed are much more sensitive to insulin as compared to wild-type mice. All together, our data indicate that *Cox6a2* is a thrifty gene which protects animals from excessive body weight loss during short-term fasting.

Discussion

The thrifty genotype hypothesis that was proposed about 50 years ago (NEEL, 1962), has been much debated over the past few years (Benyshek and Watson, 2006; Speakman, 2006; Speakman, 2007; Speakman, 2008). A first argument against the concept is that periods of famine have not been as frequent as first suggested, occurring only once every 100 years (Speakman, 2006). Second, the excess mortality rates during famines are too low to account for significant Darwinian selection and -more importantly- affect almost exclusively the very old and very young, instead of young, reproductive adults. Third, in some studies the BMI of individuals of modern hunter-gatherer and subsistence agriculture communities is low (between 17 and 21) despite being in non-famine conditions (Speakman, 2007), while such individuals should have become obese when they were selected for their thriftyness. Finally, despite 50 years of intensive research, only very few potential thrifty genes were proposed (Auwerx, 1999; Tabarin et al., 2005). Recently, it has been suggested that instead of looking for famine genes, the focus should be on genes that regulate the metabolic processes that promote survival in response to short-term, seasonally related food shortages, for which nearly all the animal kingdom is well adapted (Grant, 2006), and which have occurred for a much longer time period than the human famines. Analysis of all publically available DNA sequences of the *Cox6a1* and *Cox6a2* genes, indicates that *Cox6a2* has diverged from *Cox6a1* at an early time point in mammalian evolution (Figure S6), when enhanced survival during seasonal variations in food supply, may have been a major driving force for selection.

Our study provides evidence that *Cox6a2* qualifies as a thrifty gene in mice because: 1) Cox6a2$^{-/-}$ mice lose substantially more weight after a short period of fasting compared to wild-type mice, 2) during fasting Cox6a2 mRNA expression in slow-oxidative skeletal muscle of wild-type mice is significantly upregulated, 3) Cox6a2$^{-/-}$ mice have increased energy expenditure and thermogenesis compared to wild-type mice, 4) Cox6a2$^{-/-}$ mice are protected against high fat diet-induced obesity as a result of decreased energy efficiency and fat storage capacity, and 5) contrary to wild-type mice, Cox6a2$^{-/-}$ mice do not become glucose intolerant nor insulin resistant when fed a HFD for prolonged periods.

One of the main findings of this study is that disruption of the *Cox6a2* gene in mice protects against HFD-induced obesity, glucose intolerance and insulin resistance. These dramatic phenotypic differences from wild-type animals are best explained by an outspoken leanness, which is the result of a significant drop in triglyceride stores in white adipose tissue. Arguments for this interpretation is the decrease in total fat content, the significantly smaller adipocyte cell size and the lower circulating lipid levels in HFD-fed Cox6a2$^{-/-}$ mice, which –in turn- could partly explain increased sensitivity to insulin.

CoxVIaH deficiency in the mouse resulted in significantly increased energy expenditure and thermogenesis. We ascribe this to an increase in expression of uncoupling proteins (UCP2 and, to a lesser extent, UCP1). For several years, protective effects against obesity have been assigned to uncoupling proteins (Clapham et al., 2000; Horvath et al., 2003; Li et al., 2000; Choi et al., 2007). The epitome, UCP1, is expressed in brown adipose tissue

where it generates heat by uncoupling the mitochondrial proton gradient from ATP production. The exact physiological role of UCP2 and 3, which are more ubiquitously expressed, is still under debate (Brand and Esteves, 2005; Krauss et al., 2005), partly because both UCP2 and UCP3 knockout mice respond normally to cold exposure and are not obese, at least at room temperature (Arsenijevic et al., 2000; Gong et al., 2000; Vidal-Puig et al., 2000). However, it was suggested that UCP2 as well as UCP3 may well be thermogenic when fully activated by endogenous or exogenous effectors (Brand and Esteves, 2005). Interestingly, expression of UCPs was not only induced in skeletal muscle and heart of $Cox6a2^{-/-}$ mice, but also in brown and white adipose tissue. This argues that a crosstalk exists between skeletal muscle and WAT, as was also proposed in mice with a skeletal muscle spefic overexpression of UCP1 (Neschen et al., 2008). These mice are lean with enhanced insulin sensitivity, partly because of enhanced glucose uptake in adipose tissue. It was suggested that the release of "myokines" such as interleukin-6 (IL-6) from skeletal muscle might be responsible for this crosstalk. IL-6 has been proposed to mediate anti-inflammatory effects during exercise, which may protect against insulin resistance (Pedersen et al., 2003; Scheele et al., 2009). In mice with a skeletal muscle-specific PGC-1α deficiency, IL-6-mediated communication between skeletal muscles and pancreatic beta cells was shown to be responsible for the impaired insulin secretion in these mice (Handschin et al., 2007).

Although CoxVIaH has been proposed to be involved in thermogenesis at rest (Rohdich and Kadenbach, 1993; Lowell and Spiegelman, 2000), we found

that mice lacking this subunit actually have increased thermogenesis. We therefore hypothesize that the intrinsic uncoupling activity of CoxVIaH is compensated for by extrinsic uncoupling via UCPs, which increase thermogenesis more constitutively (Figure 7). Therefore, we believe that increased uncoupling via UCPs is the main reason for the observed protection against obesity. Our mouse model thus further corroborates the idea that increasing energy expenditure via uncoupling of ATP synthesis may be an effective method for reducing body weight.

As is proposed in our model for the lean and diabetes/obesity resistant phenotype (Figure 7), the most likely molecular mechanism by which CoxVIaH-deficiency induces expression of UCPs is dual: (i) increase in expression of the transcription factors PGC-1α and PPARα and (ii) via an increase in ROS generation. Indeed, we found elevated ROS levels in skeletal muscle of Cox6a2$^{-/-}$ mice, confirming the hypothesis that proton pump slipping protects against the formation of ROS in the mitochondria (Papa et al., 1997). The fact that we observe the biggest changes in diaphragm, the muscle with the highest oxidative capacity as assessed by citrate synthase activity (Delp and Duan, 1996; Mattson et al., 2002), suggests that the ablation of the CoxVIaH subunit mainly affects oxidative muscles. In agreement with this idea is that expression of the nuclear encoded subunits of the respiratory chain is significantly upregulated in muscles of Cox6a2$^{-/-}$ mice (Figures 4A, 4B and 4C). Again, the effect was more outspoken in diaphragm than in gastrocnemius muscle (Figure 4C). This increase in expression of respiratory chain genes suggests that there is a global

compensatory mechanism, especially in oxidative muscles, to overcome the complete knockout of the CoxVIaH subunit of complex IV. Interestingly, a similar small, but general induction of genes involved in oxidative phosphorylation was seen in mice treated with the PGC-1α activator resveratrol, which protected these mice against obesity and insulin resistance (Lagouge et al., 2006), while in diabetic or insulin resistant human subjects (Mootha et al., 2003; Patti et al., 2003) or mice (Yechoor et al., 2002), a coordinated downregulation of these genes was found. Mice with a tissue-specific knokcout of the mitochondrial flavoprotein apoptosis inducing factor (AIF) also showed a small and coordinate downregulation of respiratory chain genes (Pospisilik et al., 2007). These mice however, despite having impaired complex I and complex IV activities, were protected against obesity and diabetes.

Another possible compensation mechanism that we observed was the switch of skeletal muscle fibers towards a more oxidative profile in Cox6a2$^{-/-}$ mice resulting in skeletal muscle that was better resistant to fatigue. This result was rather surprising, since decreased muscle performance was seen in mice with a skeletal muscle-specific knockout of *Cox10*, which is an essential assembly factor of complex IV. The *Cox10*$^{musc-/-}$ mice show a severe, progressive myopathy which results in premature death at 3 to 4 months of age (Diaz et al., 2005). This phenotype could be improved by activation of the PPAR/PGC-1α pathway either by overexpression of PGC-1α or by treatment with the PPAR panagonist bezafibrate (Wenz et al., 2008). In contrast to the Cox6a2$^{-/-}$ mice, *Cox10*$^{musc-/-}$ mice displayed a severe reduction in skeletal muscle ATP content. Thus, the

phenotypic abnormalities in Cox6a2$^{-/-}$ mice are more subtle than a general respiratory chain defect and seem regulatory in terms of coupling efficiency to regulate basal energy expenditure and fat storage efficiency of food intake. This subtle change may be supported by compensation at the level of CoxVIaL, general improvement of oxidative skeletal muscle function, fiber type switch and enhanced sensitivity to insulin.

It seems surprising that skeletal muscles which generate more ROS would display increased insulin sensitivity and muscle performance. Especially since elevated ROS levels have repeatidly been associated with mitochondrial dysfunction and insulin resistance (Houstis et al., 2006; Lowell and Shulman, 2005; Petersen et al., 2003). However, recent studies argue against the causative role of mitochondrial dysfunction in the development of obesity and insulin resistance (Hancock et al., 2008; Pospisilik et al., 2007) and it has been suggested that mitochondrial dysfunction might be a consequence rather than a cause of these conditions (Bonnard et al., 2008). It is also becoming clear that ROS play a role in the regulation of cell signaling. For instance, it has been shown that moderate physical exercise results in increased muscle ROS generation followed by induction of endogenous antioxidant defense mechanisms (Gomez-Cabrera et al., 2008). Moreover, a model was proposed in which ROS signaling in response to exercise would result in the release of IL-6 from skeletal muscle which, as mentioned earlier, has anti-inflammatory effects and may protect against insulin resistance (Pedersen et al., 2003; Scheele et al., 2009). In contects other than exercise, however, IL-6 has been shown to have

proinflammatory effects. The exact role of IL-6 therefore remains controversial (Kristiansen and Mandrup-Poulsen, 2005).

Together, our data strongly support the idea that *Cox6a2* contributed to mammalian fitness as a thrifty gene that plays a central role in the economy of whole-body energy metabolism. In agreement with this idea, we found that animals that do not express this gene survive less than wild-type animals when fasted. The other side of the phenotypic coin, such animals are -when exposed chronically to calorie-dense diet, completely protected against obesity and glucose intolerance. As the *Cox6a2* gene is highly conserved in all known mammals, we suggest that our data support the idea that *Cox6a2* gene and its product(s) could become a novel target for pharmacological treatment of obesity and insulin resistance.

Experimental procedures

Animals and diet

Mice deficient in the *Cox6a2* gene were generated as previously described (Radford et al., 2002). Age- and sex-matched C57BL/6J mice were used as controls. Mice were fed a regular rodent diet (R/M-H, Ssniff, Soest, Germany). For high-fat diet studies, mice were given a diet containing 45% fat (D12451, Research Diets Inc., New Brunswick, USA) starting from 6 weeks of age, unless otherwise stated. Body weight was measured weekly. Animals were kept on a 12 hr light / 12 hr dark cycle at 20°C according to the guidelines approved by the Katholieke Universiteit Leuven animal welfare committee and the Institutional Animal Care and Research Advisory Committee of the University of Texas Southwestern Medical Center. For body temperature measurements, rectal temperature was measured at roomtemperature (time 0) using a DT-610B thermocouple thermometer (ShenZhen Everbest Machinery Industry CO.,Ltd, Shiyan, China). Mice were subsequently deprived of food, caged individually, and transferred to a cold room (4°C). Rectal temperature was then measured every hour for three hours. For the fasting experiment, mice were deprived of food, and caged individually early into the light cycle (8 am). Body weight was then followed for 36 hours.

Adipocyte size

The mean adipocyte size of subcutanous and gonadal WAT was determined by computer-assisted image analysis of adipose tissue sections stained with hematoxylin and eosin as described previously (Lijnen et al., 2006).

Glucose tolerance tests

Following an overnight fast, mice were injected with glucose (2.5 mg/g) in the intraperitoneal cavity. Blood samples were drawn from the tail vein at the indicated time points and glucose concentrations were measured using a Glucocard Memory PC (Arkray, Inc., Kyoto, Japan) glucometer.

Hyperinsulinemic, euglycemic clamps

Clamps were performed as described earlier (den Boer et al., 2006), with modifications. Briefly, after an overnight fast mice were sedated and a canula was placed in the tail vein. A basal infusion containing 1-^{14}C-glucose was subsequently injected for 1 hour at a speed of 50 µl/h. Blood samples were taken after 50 and 60 min for glucose and insulin measurement and tracer dilution. Next, a 30 µl bolus of 100 mU/ml of insulin (Actrapid, Novo Nordisk) was injected, followed by infusion of an hyperinsulinemic solution containing 1-^{14}C-glucose at a speed of 50 µl/h. After insulin infusion, blood glucose was measured at 5, 10, 15, 20, 30, 40, 50, 60, 70, 80 and 90 min. At these time points, a 12.5% glucose solution was injected in order to maintain basal glucose levels. For the estimation of insulin-stimulated glucose transport into different tissues, 2-deoxy-^{3}H-glucose was administered as a bolus at 50 min after the start of the insulin infusion. At 70,

80 and 90 min after the start of the insulin infusion, blood samples were taken for insulin measurement. After the last blood sample was taken, mice were sacrificed by cervical dyslocation and tissues were immediately isolated, snap frozen in liquid nitrogen and stored at -80°C until further analysis.

Indirect calorimetry

Utilizing the Comprehensive Lab Animal Monitoring System (CLAMS; Columbus Instruments, Columbus, Ohio), *in vivo* metabolic rates were measured in 2 to 4 months old male WT and Cox6a2$^{-/-}$ mice fed a regular diet. The metabolic studies were undertaken as previously described (Lee et al., 2006; Kublaoui et al., 2006).

Quantitative RT-PCR

Quantitative RT-PCR was performed as described (Ivarsson et al., 2005). Gene expression was normalised to RNA Pol II or beta actin expression and the expression level for each gene in WT mice fed a regular diet was set at 1.0. Primer and probe sequences are summarized in Supplementary Table X.

Assessment of Reactive Oxygen Species (ROS) levels

Utilizing the fluorescent probe dihydroethidium (DHE; Molecular Probes/Invitrogen, Carlsbad, California) *in situ* assessment of ROS levels within the diaphragm and hindlimbs of WT and Cox6a2$^{-/-}$ mice were undertaken. The diaphragm and hindlimbs of 2 to 4 months old male mice were harvested and cryopreserved. Multiple frozen sections (6 μm in thickness, n = 6 in each group) from each muscle group were cut onto glass slides and then incubated with 2 μM

DHE in a light-restricted, humidified chamber at 37°C for 30 min. A control set of slides was incubated with a PBS-based vehicle without DHE under similar conditions. Upon completion of the incubation period, vectashield (Vector Laboratories; Burlingame, California) and coverslips were placed over the tissue sections. Assessment of ROS levels was performed utilizing a photomicroscope equipped with fluorescence (Leica DM-2000; Wetzlar, Germany). Quantification of the ROS levels on a tissue section was undertaken by measuring the number of DHE positive nuclei per unit area.

Metachromatic fiber typing of skeletal myofibers

The gastrocnemius muscles from WT and Cox6a2$^{-/-}$ mice were harvested, fixed in 10% formalin and cryopreserved. Subsequently, fiber typing was performed utilizing a metachromatic dye-ATPase assay as previously described (Wu et al., 2001; Ogilvie and Feeback, 1990).

Myofiber cross-sectional area

Cross-sectional areas of skeletal muscle fibers were quantified using NIH software ImageJ 1.37V. The software was used to draw boundaries and calculate areas for any individual cell within a snapshot. The appropriate square micron scale was set up prior to measuring the area. From each snapshot, multiple cells were measured for each of the three fiber types, and multiple snapshots were used per mouse.

Statistical analysis

All data are shown as means ± SEM. Differences between experimental groups were determined by the unpaired, two-tailed Student's t-test or the Mann-Whitney rank-sum test. A p-value < 0.05 was considered to indicate statistical significance.

Acknowledgements

The authors would like to thank Prof. J. Van Sande and Prof. J. Dumont (Université Libre De Bruxelles) for measuring plasma thyroid hormone and thyrotropin levels. This work was supported by grants of the Katholieke Universiteit Leuven (GOA 2004/11, GOA 2008/16 and SymBioSys), the Belgian Ministry for Science Policy (IUAP P6/40), and the European Union (EURODIA FP6-518153).

Reference List

Anthony,G., Reimann,A., and Kadenbach,B. (1993). Tissue-specific regulation of bovine heart cytochrome-c oxidase activity by ADP via interaction with subunit VIa. Proc. Natl. Acad. Sci. U. S. A *90*, 1652-1656.

Arsenijevic,D., Onuma,H., Pecqueur,C., Raimbault,S., Manning,B.S., Miroux,B., Couplan,E., ves-Guerra,M.C., Goubern,M., Surwit,R., Bouillaud,F., Richard,D., Collins,S., and Ricquier,D. (2000). Disruption of the uncoupling protein-2 gene in mice reveals a role in immunity and reactive oxygen species production. Nat. Genet. *26*, 435-439.

Auwerx,J. (1999). PPARgamma, the ultimate thrifty gene. Diabetologia *42*, 1033-1049.

Benyshek,D.C. and Watson,J.T. (2006). Exploring the thrifty genotype's food-shortage assumptions: a cross-cultural comparison of ethnographic accounts of food security among foraging and agricultural societies. Am. J. Phys. Anthropol. *131*, 120-126.

Bonnard,C., Durand,A., Peyrol,S., Chanseaume,E., Chauvin,M.A., Morio,B., Vidal,H., and Rieusset,J. (2008). Mitochondrial dysfunction results from oxidative stress in the skeletal muscle of diet-induced insulin-resistant mice. J. Clin. Invest *118*, 789-800.

Brand,M.D., Affourtit,C., Esteves,T.C., Green,K., Lambert,A.J., Miwa,S., Pakay,J.L., and Parker,N. (2004a). Mitochondrial superoxide: production, biological effects, and activation of uncoupling proteins. Free Radic. Biol. Med. *37*, 755-767.

Brand,M.D., Buckingham,J.A., Esteves,T.C., Green,K., Lambert,A.J., Miwa,S., Murphy,M.P., Pakay,J.L., Talbot,D.A., and Echtay,K.S. (2004b). Mitochondrial superoxide and aging: uncoupling-protein activity and superoxide production. Biochem. Soc. Symp. 203-213.

Brand,M.D. and Esteves,T.C. (2005). Physiological functions of the mitochondrial uncoupling proteins UCP2 and UCP3. Cell Metab *2*, 85-93.

Choi,C.S., Fillmore,J.J., Kim,J.K., Liu,Z.X., Kim,S., Collier,E.F., Kulkarni,A., Distefano,A., Hwang,Y.J., Kahn,M., Chen,Y., Yu,C., Moore,I.K., Reznick,R.M., Higashimori,T., and Shulman,G.I. (2007). Overexpression of uncoupling protein 3 in skeletal muscle protects against fat-induced insulin resistance. J. Clin. Invest *117*, 1995-2003.

Clapham,J.C., Arch,J.R., Chapman,H., Haynes,A., Lister,C., Moore,G.B., Piercy,V., Carter,S.A., Lehner,I., Smith,S.A., Beeley,L.J., Godden,R.J.,

Herrity,N., Skehel,M., Changani,K.K., Hockings,P.D., Reid,D.G., Squires,S.M., Hatcher,J., Trail,B., Latcham,J., Rastan,S., Harper,A.J., Cadenas,S., Buckingham,J.A., Brand,M.D., and Abuin,A. (2000). Mice overexpressing human uncoupling protein-3 in skeletal muscle are hyperphagic and lean. Nature *406*, 415-418.

Crawford,D., Jeffery,R.W., and French,S.A. (2000). Can anyone successfully control their weight? Findings of a three year community-based study of men and women. Int. J. Obes. Relat Metab Disord. *24*, 1107-1110.

Delp,M.D. and Duan,C. (1996). Composition and size of type I, IIA, IID/X, and IIB fibers and citrate synthase activity of rat muscle. J. Appl. Physiol *80*, 261-270.

den Boer,M.A., Voshol,P.J., Schroder-van der Elst JP, Korsheninnikova,E., Ouwens,D.M., Kuipers,F., Havekes,L.M., and Romijn,J.A. (2006). Endogenous interleukin-10 protects against hepatic steatosis but does not improve insulin sensitivity during high-fat feeding in mice. Endocrinology *147*, 4553-4558.

Diaz,F., Thomas,C.K., Garcia,S., Hernandez,D., and Moraes,C.T. (2005). Mice lacking COX10 in skeletal muscle recapitulate the phenotype of progressive mitochondrial myopathies associated with cytochrome c oxidase deficiency. Hum. Mol. Genet. *14*, 2737-2748.

Echtay,K.S., Murphy,M.P., Smith,R.A., Talbot,D.A., and Brand,M.D. (2002a). Superoxide activates mitochondrial uncoupling protein 2 from the matrix side. Studies using targeted antioxidants. J. Biol. Chem. *277*, 47129-47135.

Echtay,K.S., Roussel,D., St-Pierre,J., Jekabsons,M.B., Cadenas,S., Stuart,J.A., Harper,J.A., Roebuck,S.J., Morrison,A., Pickering,S., Clapham,J.C., and Brand,M.D. (2002b). Superoxide activates mitochondrial uncoupling proteins. Nature *415*, 96-99.

Frank,V. and Kadenbach,B. (1996). Regulation of the H+/e- stoichiometry of cytochrome c oxidase from bovine heart by intramitochondrial ATP/ADP ratios. FEBS Lett. *382*, 121-124.

Gates,A.C., Bernal-Mizrachi,C., Chinault,S.L., Feng,C., Schneider,J.G., Coleman,T., Malone,J.P., Townsend,R.R., Chakravarthy,M.V., and Semenkovich,C.F. (2007). Respiratory uncoupling in skeletal muscle delays death and diminishes age-related disease. Cell Metab *6*, 497-505.

Gomez-Cabrera,M.C., Domenech,E., and Vina,J. (2008). Moderate exercise is an antioxidant: upregulation of antioxidant genes by training. Free Radic. Biol. Med. *44*, 126-131.

Gong,D.W., Monemdjou,S., Gavrilova,O., Leon,L.R., Marcus-Samuels,B., Chou,C.J., Everett,C., Kozak,L.P., Li,C., Deng,C., Harper,M.E., and

Reitman,M.L. (2000). Lack of obesity and normal response to fasting and thyroid hormone in mice lacking uncoupling protein-3. J. Biol. Chem. *275*, 16251-16257.

Grant,P.J. (2006). Obesity, diabetes and cardiovascular disease: is the fat lady singing? Diab. Vasc. Dis. Res. *3*, 5-6.

Hancock,C.R., Han,D.H., Chen,M., Terada,S., Yasuda,T., Wright,D.C., and Holloszy,J.O. (2008). High-fat diets cause insulin resistance despite an increase in muscle mitochondria. Proc. Natl. Acad. Sci. U. S. A *105*, 7815-7820.

Handschin,C., Choi,C.S., Chin,S., Kim,S., Kawamori,D., Kurpad,A.J., Neubauer,N., Hu,J., Mootha,V.K., Kim,Y.B., Kulkarni,R.N., Shulman,G.I., and Spiegelman,B.M. (2007). Abnormal glucose homeostasis in skeletal muscle-specific PGC-1alpha knockout mice reveals skeletal muscle-pancreatic beta cell crosstalk. J. Clin. Invest *117*, 3463-3474.

Horvath,T.L., Diano,S., Miyamoto,S., Barry,S., Gatti,S., Alberati,D., Livak,F., Lombardi,A., Moreno,M., Goglia,F., Mor,G., Hamilton,J., Kachinskas,D., Horwitz,B., and Warden,C.H. (2003). Uncoupling proteins-2 and 3 influence obesity and inflammation in transgenic mice. Int. J. Obes. Relat Metab Disord. *27*, 433-442.

Houstis,N., Rosen,E.D., and Lander,E.S. (2006). Reactive oxygen species have a causal role in multiple forms of insulin resistance. Nature *440*, 944-948.

Ivarsson,R., Quintens,R., Dejonghe,S., Tsukamoto,K., in 't Veld,P., Renstrom,E., and Schuit,F.C. (2005). Redox control of exocytosis: regulatory role of NADPH, thioredoxin, and glutaredoxin. Diabetes *54*, 2132-2142.

Kadenbach,B., Barth,J., Akgun,R., Freund,R., Linder,D., and Possekel,S. (1995). Regulation of mitochondrial energy generation in health and disease. Biochim. Biophys. Acta *1271*, 103-109.

Krauss,S., Zhang,C.Y., and Lowell,B.B. (2005). The mitochondrial uncoupling-protein homologues. Nat. Rev. Mol. Cell Biol. *6*, 248-261.

Kristiansen,O.P. and Mandrup-Poulsen,T. (2005). Interleukin-6 and diabetes: the good, the bad, or the indifferent? Diabetes *54 Suppl 2*, S114-S124.

Kublaoui,B.M., Holder,J.L., Jr., Tolson,K.P., Gemelli,T., and Zinn,A.R. (2006). SIM1 overexpression partially rescues agouti yellow and diet-induced obesity by normalizing food intake. Endocrinology *147*, 4542-4549.

Lagouge,M., Argmann,C., Gerhart-Hines,Z., Meziane,H., Lerin,C., Daussin,F., Messadeq,N., Milne,J., Lambert,P., Elliott,P., Geny,B., Laakso,M., Puigserver,P., and Auwerx,J. (2006). Resveratrol improves mitochondrial function and protects against metabolic disease by activating SIRT1 and PGC-1alpha. Cell *127*, 1109-1122.

Lee,C.H., Olson,P., Hevener,A., Mehl,I., Chong,L.W., Olefsky,J.M., Gonzalez,F.J., Ham,J., Kang,H., Peters,J.M., and Evans,R.M. (2006). PPARdelta regulates glucose metabolism and insulin sensitivity. Proc. Natl. Acad. Sci. U. S. A *103*, 3444-3449.

Lee,F.Y., Li,Y., Zhu,H., Yang,S., Lin,H.Z., Trush,M., and Diehl,A.M. (1999). Tumor necrosis factor increases mitochondrial oxidant production and induces expression of uncoupling protein-2 in the regenerating mice [correction of rat] liver. Hepatology *29*, 677-687.

Li,B., Nolte,L.A., Ju,J.S., Han,D.H., Coleman,T., Holloszy,J.O., and Semenkovich,C.F. (2000). Skeletal muscle respiratory uncoupling prevents diet-induced obesity and insulin resistance in mice. Nat. Med. *6*, 1115-1120.

Lijnen,H.R., Christiaens,V., Scroyen,I., Voros,G., Tjwa,M., Carmeliet,P., and Collen,D. (2006). Impaired adipose tissue development in mice with inactivation of placental growth factor function. Diabetes *55*, 2698-2704.

Lowell,B.B. and Shulman,G.I. (2005). Mitochondrial dysfunction and type 2 diabetes. Science *307*, 384-387.

Lowell,B.B. and Spiegelman,B.M. (2000). Towards a molecular understanding of adaptive thermogenesis. Nature *404*, 652-660.

Mattson,J.P., Miller,T.A., Poole,D.C., and Delp,M.D. (2002). Fiber composition and oxidative capacity of hamster skeletal muscle. J. Histochem. Cytochem. *50*, 1685-1692.

Mootha,V.K., Lindgren,C.M., Eriksson,K.F., Subramanian,A., Sihag,S., Lehar,J., Puigserver,P., Carlsson,E., Ridderstrale,M., Laurila,E., Houstis,N., Daly,M.J., Patterson,N., Mesirov,J.P., Golub,T.R., Tamayo,P., Spiegelman,B., Lander,E.S., Hirschhorn,J.N., Altshuler,D., and Groop,L.C. (2003). PGC-1alpha-responsive genes involved in oxidative phosphorylation are coordinately downregulated in human diabetes. Nat. Genet. *34*, 267-273.

NEEL,J.V. (1962). Diabetes mellitus: a "thrifty" genotype rendered detrimental by "progress"? Am. J. Hum. Genet. *14*, 353-362.

Neschen,S., Katterle,Y., Richter,J., Augustin,R., Scherneck,S., Mirhashemi,F., Schurmann,A., Joost,H.G., and Klaus,S. (2008). Uncoupling protein 1 expression in murine skeletal muscle increases AMPK activation, glucose turnover, and insulin sensitivity in vivo. Physiol Genomics *33*, 333-340.

Ogilvie,R.W. and Feeback,D.L. (1990). A metachromatic dye-ATPase method for the simultaneous identification of skeletal muscle fiber types I, IIA, IIB and IIC. Stain Technol. *65*, 231-241.

Papa,S., Guerrieri,F., and Capitanio,N. (1997). A possible role of slips in cytochrome C oxidase in the antioxygen defense system of the cell. Biosci. Rep. *17*, 23-31.

Patti,M.E., Butte,A.J., Crunkhorn,S., Cusi,K., Berria,R., Kashyap,S., Miyazaki,Y., Kohane,I., Costello,M., Saccone,R., Landaker,E.J., Goldfine,A.B., Mun,E., DeFronzo,R., Finlayson,J., Kahn,C.R., and Mandarino,L.J. (2003). Coordinated reduction of genes of oxidative metabolism in humans with insulin resistance and diabetes: Potential role of PGC1 and NRF1. Proc. Natl. Acad. Sci. U. S. A *100*, 8466-8471.

Pedersen,B.K., Steensberg,A., Keller,P., Keller,C., Fischer,C., Hiscock,N., van,H.G., Plomgaard,P., and Febbraio,M.A. (2003). Muscle-derived interleukin-6: lipolytic, anti-inflammatory and immune regulatory effects. Pflugers Arch. *446*, 9-16.

Petersen,K.F., Befroy,D., Dufour,S., Dziura,J., Ariyan,C., Rothman,D.L., DiPietro,L., Cline,G.W., and Shulman,G.I. (2003). Mitochondrial dysfunction in the elderly: possible role in insulin resistance. Science *300*, 1140-1142.

Polak,P., Cybulski,N., Feige,J.N., Auwerx,J., Ruegg,M.A., and Hall,M.N. (2008). Adipose-specific knockout of raptor results in lean mice with enhanced mitochondrial respiration. Cell Metab *8*, 399-410.

Pospisilik,J.A., Knauf,C., Joza,N., Benit,P., Orthofer,M., Cani,P.D., Ebersberger,I., Nakashima,T., Sarao,R., Neely,G., Esterbauer,H., Kozlov,A., Kahn,C.R., Kroemer,G., Rustin,P., Burcelin,R., and Penninger,J.M. (2007). Targeted deletion of AIF decreases mitochondrial oxidative phosphorylation and protects from obesity and diabetes. Cell *131*, 476-491.

Puigserver,P., Wu,Z., Park,C.W., Graves,R., Wright,M., and Spiegelman,B.M. (1998). A cold-inducible coactivator of nuclear receptors linked to adaptive thermogenesis. Cell *92*, 829-839.

Radford,N.B., Wan,B., Richman,A., Szczepaniak,L.S., Li,J.L., Li,K., Pfeiffer,K., Schagger,H., Garry,D.J., and Moreadith,R.W. (2002). Cardiac dysfunction in mice lacking cytochrome-c oxidase subunit VIaH. Am. J. Physiol Heart Circ. Physiol *282*, H726-H733.

Reitman,M.L. (2002). Metabolic lessons from genetically lean mice. Annu. Rev. Nutr. *22*, 459-482.

Rohdich,F. and Kadenbach,B. (1993). Tissue-specific regulation of cytochrome c oxidase efficiency by nucleotides. Biochemistry *32*, 8499-8503.

Scheele,C., Nielsen,S., and Pedersen,B.K. (2009). ROS and myokines promote muscle adaptation to exercise. Trends Endocrinol. Metab *20*, 95-99.

Sokolovic,M., Wehkamp,D., Sokolovic,A., Vermeulen,J., Gilhuijs-Pederson,L.A., van Haaften,R.I., Nikolsky,Y., Evelo,C.T., van Kampen,A.H., Hakvoort,T.B., and Lamers,W.H. (2007). Fasting induces a biphasic adaptive metabolic response in murine small intestine. BMC. Genomics *8*, 361.

Speakman,J.R. (2007). A nonadaptive scenario explaining the genetic predisposition to obesity: the "predation release" hypothesis. Cell Metab *6*, 5-12.

Speakman,J.R. (2008). Thrifty genes for obesity, an attractive but flawed idea, and an alternative perspective: the 'drifty gene' hypothesis. Int. J. Obes. (Lond) *32*, 1611-1617.

Speakman,J.R. (2006). Thrifty genes for obesity and the metabolic syndrome--time to call off the search? Diab. Vasc. Dis. Res. *3*, 7-11.

Taanman,J.W., Hall,R.E., Tang,C., Marusich,M.F., Kennaway,N.G., and Capaldi,R.A. (1993). Tissue distribution of cytochrome c oxidase isoforms in mammals. Characterization with monoclonal and polyclonal antibodies. Biochim. Biophys. Acta *1225*, 95-100.

Tabarin,A., Diz-Chaves,Y., Carmona,M.C., Catargi,B., Zorrilla,E.P., Roberts,A.J., Coscina,D.V., Rousset,S., Redonnet,A., Parker,G.C., Inoue,K., Ricquier,D., Penicaud,L., Kieffer,B.L., and Koob,G.F. (2005). Resistance to diet-induced obesity in mu-opioid receptor-deficient mice: evidence for a "thrifty gene". Diabetes *54*, 3510-3516.

Tsukihara,T., Aoyama,H., Yamashita,E., Tomizaki,T., Yamaguchi,H., Shinzawa-Itoh,K., Nakashima,R., Yaono,R., and Yoshikawa,S. (1996). The whole structure of the 13-subunit oxidized cytochrome c oxidase at 2.8 A. Science *272*, 1136-1144.

Vidal-Puig,A.J., Grujic,D., Zhang,C.Y., Hagen,T., Boss,O., Ido,Y., Szczepanik,A., Wade,J., Mootha,V., Cortright,R., Muoio,D.M., and Lowell,B.B. (2000). Energy metabolism in uncoupling protein 3 gene knockout mice. J. Biol. Chem. *275*, 16258-16266.

Wenz,T., Diaz,F., Spiegelman,B.M., and Moraes,C.T. (2008). Activation of the PPAR/PGC-1alpha pathway prevents a bioenergetic deficit and effectively improves a mitochondrial myopathy phenotype. Cell Metab *8*, 249-256.

Wu,H., Rothermel,B., Kanatous,S., Rosenberg,P., Naya,F.J., Shelton,J.M., Hutcheson,K.A., DiMaio,J.M., Olson,E.N., Bassel-Duby,R., and Williams,R.S. (2001). Activation of MEF2 by muscle activity is mediated through a calcineurin-dependent pathway. EMBO J. *20*, 6414-6423.

Yang,S., Zhu,H., Li,Y., Lin,H., Gabrielson,K., Trush,M.A., and Diehl,A.M. (2000). Mitochondrial adaptations to obesity-related oxidant stress. Arch. Biochem. Biophys. *378*, 259-268.

Yechoor,V.K., Patti,M.E., Saccone,R., and Kahn,C.R. (2002). Coordinated patterns of gene expression for substrate and energy metabolism in skeletal muscle of diabetic mice. Proc. Natl. Acad. Sci. U. S. A *99*, 10587-10592.

Zanetti,M., d'Uscio,L.V., Peterson,T.E., Katusic,Z.S., and O'Brien,T. (2005). Analysis of superoxide anion production in tissue. Methods Mol. Med. *108*, 65-72.

Figure legends

Figure 1. Accelerated body weight loss and increased cold-induced thermogenesis in fasted Cox6a2$^{-/-}$ mice

(A-B) Male (A) (n= 10) and female (B) (n = 3-7) mice were deprived of food at 7 am. Throughout the experiment, they had unlimited access to water. Body weight was measured for 36 h. Note that 2 out of 10 male Cox6a2$^{-/-}$ mice were eliminated from the experiment after 24 h.

(C) Cox6a2 mRNA expression in skeletal muscles of fed and 16 h fasted mice. Gastrocn. = gastrocnemius muscle.

(D-E) Mice fed a regular diet (D) or a HFD (E) were deprived of food, exposed to cold and core body temperatures were measured every hour for three hours (n = 5-9 for RD, n = 5-11 for HFD). *p < 0.05, **p < 0.01, ***p < 0.001. In all panels, data represent mean ± SEM.

Figure 2. Increased energy expenditure in Cox6a2$^{-/-}$ mice

(A-E) Oxygen consumption (A), respiratory exchange ratio (B), heat generation (C), and spontaneous activity (D-E) measured in mice of 12-16 weeks old (n = 4-5). Measurements were performed over a 3-day period. Gray shades in A and B indicate dark cycles. *p < 0.05. In all panels, data represent mean ± SEM.

Figure 3. Increased UCP2 mRNA expression and ROS production in metabolically active tissues of Cox6a2$^{-/-}$ mice

(A) Quantitative RT-PCRs were performed on cDNA from gastrocnemius muscle, diaphragm, soleus muscle, heart, WAT, and BAT (n = 3-5). Gene expression was normalized to RNA Pol II as a reference gene and expression in WT mice was set at 1.0 for each individual gene. ND = Not detected.

(B) Measurement of steady state ROS levels by DHE staining. Left panel shows representative images of DHE stained sections of the diaphragm

(upper) and hindlimbs (lower) of WT and Cox6a2$^{-/-}$ mice. Right panel shows the quantification of the number of positive myocytes stained with DHE (n = 6). *p < 0.05, **p < 0.01, ***p < 0.001. In all panels, data represent mean ± SEM.

Figure 4. Increased expression of oxidative myofiber markers and genes involved in electron transport in Cox6a2$^{-/-}$ mice

(A-B) GSEA enrichment score curves. Gene Set Enrichment Analysis (GSEA) of gene expression in diaphragm (A) and gastrocnemius (B) of wild-type and Cox6a2$^{-/-}$ mice on a regular diet (n = 3). Genes were ranked according to their signal-to-noise ratio after which enrichment scores were calculated. The green line represents the running enrichment score curve as it progresses along the ranked genes. Black vertical lines indicate the position of the genes in the ranked gene list. Gene sets were downloaded from the MSigDB database (http://www.broad.mit.edu/gsea/msigdb/index.jsp).

(C) Relative changes in expression of genes of the electron transport chain in diaphragm and gastrocnemius of Cox6a2$^{-/-}$ mice compared to WT mice. Horizontal bars indicate mean difference in expression. For complex IV, CoxVIaH was not taken into account for calculation of the mean difference in expression. CI, complex I; CII, complex II; CIII, complex III; CIV, complex IV; CV, complex V (ATP synthase); Cytc, cytochrome c.

(D) Gastrocnemius muscle fiber typing by metachromatic staining of myosin ATPase activity. ATPase activity stains type I fibers dark blue, type IIa fibers light blue, and type IIb fibers very light blue. Representative images of fiber typing in the gastrocnemius muscle from WT and Cox6a2$^{-/-}$ mice are shown.

(E) Quantification of muscle fiber types in gastrocnemius muscle of WT and Cox6a2$^{-/-}$ mice (n = 20-30). Note the increase in the total number of fibers in gastrocnemius muscle from Cox6a2$^{-/-}$ mice. Scale bar = 100 μm. I, IIA, and IIB refer to type I, type IIA, and type IIB fibers.

(F) Cross-sectional area of different fiber types in gastrocnemius of wild-type and Cox6a2$^{-/-}$ mice (n = 30-60). Scale bar = 100 μm. *p < 0.05. Data represent mean ± SEM.

Figure 5. Cox6a2$^{-/-}$ mice are protected against diet-induced obesity

(A) Mice were fed a regular diet or a HFD starting from 6 weeks of age (n = 5 for WT, n = 14-16 for Cox6a2$^{-/-}$ mice). Body weight was monitored weekly between 10 and 11 am.

(B) Average food intake and feeding efficiency of mice fed a HFD (n = 5).

(C) Average weight of gastrocnemius muscle, heart, liver, subcutanous WAT and gonadal WAT was measured in mice that were fed a HFD for 12 weeks (n = 5).

(D) Representatitve pictures of H&E staining of gonadal WAT of mice fed a HFD for 12 weeks.

(E) Quantification of subcutanous and gonadal WAT cell size and density (n = 5). *p < 0.05, **p < 0.01, ***p < 0.001. In all panels, data represent mean ± SEM.

Figure 6. Increased glucose tolerance and insulin sensititvity in Cox6a2$^{-/-}$ mice fed a HFD

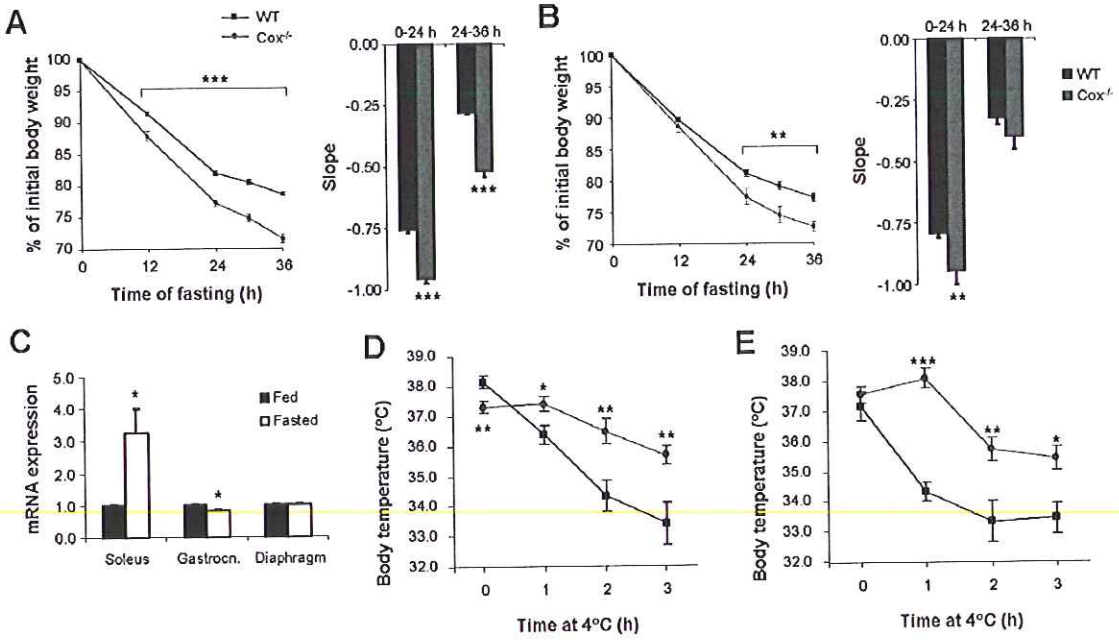
(A) After a 16-18 h fast, mice were injected with 2.5 mg/g glucose and blood glucose levels were monitored for 2 h (n = 7-9 for RD, n = 4-11 for 9 weeks of HFD, n = 3-4 for 22 weeks of HFD). Mean areas under the curve are shown on the right.

(B) Hyperinsulinemic, euglycemic clamps were performed on mice (21 weeks old) fed a HFD for 15 weeks (n = 6-8). Blood glucose levels (left panel) and glucose infusion rate (middle panel) were monitored for 90 min after administration of an hyperinsulinemic solution via the tail vein. Mean areas under the curves are shown on the right. *p < 0.05, **p < 0.01, ***p < 0.001 for effect of genotype; $^{\#}p$ < 0.05, $^{\#\#}p$ < 0.01, $^{\#\#\#}p$ < 0.001 for effect of diet. In all panels, data represent mean ± SEM.

Figure 7. Model of the role of Cox6a2$^{-/-}$ in energy homeostasis

Induction of UCPs and fiber type switch in Cox6a2$^{-/-}$ mice: Loss of intrinsic uncoupling via CoxVIaH leads to increased generation of ROS, which subsequently induces the expression/activation of UCPs. This leads to elevated energy expenditure and adaptive thermogenesis, resulting in protection against diet-induced obesity. A supplementary pathway for UCP induction may be via increased expression of PPARα and PGC-1α. The latter may also be responsible for compensatory oxidative fiber type switch and enhanced expression of respiratory chain genes.

Figure 1


A
WT
Cox-/-
% of initial body weight
Time of fasting (h)
0-24 h
24-36 h
Slope
B
C
mRNA expression
Fed
Fasted
Soleus
Gastrocn.
Diaphragm
D
Body temperature (°C)
Time at 4°C (h)
E